# Functional role of cyclic nucleotide-gated channels in rat medial vestibular nucleus neurons

Maria Vittoria Podda, Marcello D'Ascenzo, Lucia Leone, Roberto Piacentini, Gian Battista Azzena and Claudio Grassi

*Institute of Human Physiology, Medical School, Catholic University 'S. Cuore', I-00168 Rome, Italy*

**Although cyclic nucleotide-gated (CNG) channels are expressed in numerous brain areas, little information is available on their functions in CNS neurons. The aim of the present study was to define the distribution of CNG channels in the rat medial vestibular nucleus (MVN) and their possible involvement in regulating MVN neuron (MVNn) excitability. The majority of MVNn expressed both CNG1 and CNG2 A subunits. In whole-cell current-clamp experiments carried out on brainstem slices containing the MVNn, the membrane-permeant analogues of cyclic nucleotides, 8-Br-cGMP and 8-Br-cAMP (1 mM), induced membrane depolarizations (8.9 ± 0.8 and 9.2 ± 1.0 mV, respectively) that were protein kinase independent. The cGMP-induced depolarization was associated with a significant decrease in the membrane input resistance. The effects of cGMP on membrane potential were almost completely abolished by the CNG channel blockers, $Cd^{2+}$ and L-*cis*-diltiazem, but they were unaffected by blockade of hyperpolarization-activated cyclic nucleotide-gated channels. In voltage-clamp experiments, 8-Br-cGMP induced non-inactivating inward currents (−22.2 ± 3.9 pA) with an estimated reversal potential near 0 mV, which were markedly inhibited by reduction of extracellular $Na^+$ and $Ca^{2+}$ concentrations. Membrane depolarization induced by CNG channel activation increased the firing rate of MVNn without changing the action potential shape. Collectively, these findings provide novel evidence that CNG channels affect membrane potential and excitability of MVNn. Such action should have a significant impact on the function of these neurons in sensory–motor integration processes. More generally, it might represent a broad mechanism for regulating the excitability of different CNS neurons.**

(Received 7 October 2007; accepted after revision 28 November 2007; first published online 29 November 2007)
**Corresponding author** C. Grassi: Institute of Human Physiology, Medical School, Catholic University 'S. Cuore', Largo F. Vito 1, 00168 Rome, Italy. Email: grassi@rm.unicatt.it

Neurons of the vestibular nuclei contribute to the control of gaze and posture by processing multisensory signals related to head and body movements and transforming them into motor commands (Wilson *et al.* 1990). The medial vestibular nucleus neurons (MVNn) are important components of the vestibuloocular, optokinetic and vestibulo-collic reflex circuits. They integrate visual, proprioceptive and vestibular inputs and generate compensatory eye and head movements via their projections to oculomotor and neck motoneurons, respectively. MVNn fire spontaneously even in the absence of the glutamatergic and GABAergic inputs that physiologically regulate their discharge rate (Dutia *et al.* 1992; Chun *et al.* 2003). This rhythmic activity depends largely on the activation of several types of $K^+$ currents, including the voltage-gated $I_K$, the $Ca^{2+}$-dependent BK and SK currents and $I_A$-like $K^+$ currents. These currents are critical determinants of the profile of action potential repolarization and the shape and depth of after-hyperpolarization (AHP), factors that have marked effects on the interspike intervals (Johnston *et al.* 1994; Eugène *et al.* 2007; for review, see Gittis & du Lac, 2007; Straka *et al.* 2005). Important contributions in determining the activity of MVNn are also made by other ion conductances including persistent $Na^+$ currents that significantly contribute to generate a steady depolarization of the membrane potential and tonic discharge at rest. A complete picture of the different ionic conductances involved in the spontaneous firing of MVNn and the physiological signals that regulate their excitability is crucial for understanding the mechanisms underlying modulation of information processing and the final output of these neurons.

Increasing attention is now being focused on the involvement of voltage-independent channels in determining the resting potential and excitability of

 DOI: 10.1113/jphysiol.2007.146019

neurons. Our recent work has shown that the cyclic nucleotides, cGMP and cAMP, enhance MVNn excitability and increase their firing rate through a mechanism that does not depend on protein kinase activation. We suggested that these effects are mediated by cyclic nucleotide-gated (CNG) channels (Podda *et al.* 2004, 2005), a family of voltage-independent, non-selective cation channels originally identified in visual and olfactory sensory cells, where they play a critical role in the transduction of sensory stimuli (Fesenko *et al.* 1985; Dhallan *et al.* 1990; Kaupp & Seifert, 2002; Ko *et al.* 2004).

Extensive evidence has also emerged for the expression of CNG channels in several mammalian brain areas, and together with cAMP- and cGMP-dependent protein kinases, these channels are considered major biological effectors of the actions of cyclic nucleotides in the central nervous system (CNS) (el-Husseini *et al.* 1995; Kingston *et al.* 1996; Bradley *et al.* 1997; Kingston *et al.* 1999; Samanta Roy & Barnstable, 1999; Strijbos *et al.* 1999). Despite their broad distribution in the brain, very little information is available on the functional role of CNG channels in CNS neurons. Because of their high permeability to $Na^+$ and $Ca^{2+}$, they have the potential to influence numerous neuronal functions in the CNS, including cell excitability and several $Ca^{2+}$-dependent intracellular processes (Zufall *et al.* 1997).

The aim of the present study was to identify the function of CNG channels in MVNn and their potential for modulating MVNn excitability. The data reported here suggest that cGMP- and cAMP-induced activation of CNG channels in MVNn triggers an inward cationic current, which causes protein kinase-independent membrane depolarization, and that these events appear to play a key role in regulating the MVNn firing rate.

## Methods

### Ethical approval

All procedures on animals were approved by the Ethical Committee of the Catholic University, in compliance with the guidelines of the Italian Ministry of Health, the national laws on animal research (d.l. 116/92), and the EU guidelines on animal research (N. 86/609/CEE).

### Immunohistochemistry

Male Wistar rats (14–17 days old) were deeply anaesthetized by intraperitoneal injection of 0.2 ml $kg^{-1}$ of a 1 : 1 solution of xylazine (Bayer, Leverkusen, Germany) and ketamine (Virbac, Carros, France), and perfused transcardially with oxygenated Ringer solution, pH 7.3, followed by 4% freshly depolymerized paraformaldehyde in phosphate buffer solution (PBS). Brains were removed, left in the same fixative (2 h at 4°C) and cryoprotected for 36 h in 30% sucrose at 4°C. Coronal sections (30 $\mu$m-thick), cut on a vibratome (VT1000S Leica Microsystems, Nussloch, Germany), were collected freely floating and stored in antifreeze solution at −20°C until use. After 3 × 10 min rinses in PBS, the sections were incubated in a blocking solution containing 1% bovine serum albumin (BSA), 10% normal goat serum (NGS) and 0.5% Triton X-100 (TX-100) in PBS, for 1 h at room temperature (RT) and then incubated with the rabbit anti-CNG1 (Alpha Diagnostic International, San Antonio, TX, USA) or CNG2 (Alomone Laboratories, Jerusalem, Israel) antibodies diluted (1 : 30 and 1 : 60, respectively) in a solution of 1% BSA, 5% NGS and 0.3% TX-100 in PBS, for 48 h at 4°C. After rinsing in PBS, the sections were revealed with the secondary antibody donkey antirabbit Alexa Fluor 488 (1 : 1000, Invitrogen, Milan, Italy), further rinsed, and incubated with the mouse monoclonal anti-NeuN (1 : 600, Chemicon International, Temecula, CA, USA) or anti-GFAP (1 : 100, Cell Signalling Technology, Beverly, MA, USA) antibodies. Both double immunolabellings were successively revealed with goat antimouse IgG rhodamine conjugate secondary antibody (1 : 300, Chemicon). Those sections double labelled with GFAP were also stained with the nuclear marker, 4′6amidino-2-phenylindole 2 HCl (DAPI; 0.5 $\mu$g $ml^{-1}$; Invitrogen). Control sections from all specimens were obtained by omitting the primary antibody. No specific signals were ever detected. All sections were collected on glass slide and cover-slipped with ProLong gold antifade reagent (Invitrogen).

Immunostained sections were analysed by a confocal laser scanning system (TCS-SP2, Leica Microsystems, GmbH, Wetzlar, Germany) equipped with an Ar/ArKr laser and a HeNe laser for 488 nm and 543 nm excitation, respectively. The emission signals were collected by photomultipliers in two spectral windows ranging from 500 nm to 540 nm and from 560 nm to 600 nm, respectively. DAPI staining was imaged by 2-photon excitation (740 nm, <140 fs, 90 MHz) performed by a ultrafast tunable mode-locked Ti:Saffire laser (Chameleon, Coherent Inc., Santa Clara, CA, USA) and collected in a spectral window ranging from 400 nm to 480 nm.

For each analysed field, sections of Z-stack series of 5 $\mu$m-thick sections were acquired as images (512 × 512 pixels) recorded at intervals of 0.17 $\mu$m, and then projection images were created and processed using the Leica software LCS in order to optimize brightness and contrast.

### Electrophysiological experiments

**Slice preparation.** Coronal slices of the brainstem (300 $\mu$m thick) containing the MVN were prepared from 14- to 17-day-old Wistar rats using standard procedures

(Sekirnjak & du Lac, 2002; D'Ascenzo *et al.* 2007). Briefly, the animals were anaesthetized by inhalation of halothane (Sigma, Milan, Italy) and decapitated. The brain was rapidly removed and put in ice-cold cutting solution containing (mM): 120 NaCl, 3.2 KCl, 1 $KH_2PO_4$, 26 $NaHCO_3$, 2 $MgCl_2$, 1 $CaCl_2$, 10 glucose, 2 sodium pyruvate, and 0.6 ascorbic acid (pH 7.4, 95% $O_2$–5% $CO_2$). Slices were cut with a vibratome (VT1000S, Leica Microsystems) and incubated in the cutting solution at 34°C for 60 min and then at RT until use.

**Patch-clamp recordings.** Slices were transferred to a submerged recording chamber and continuously perfused with artificial cerebrospinal fluid (aCSF) containing (mM): 124 NaCl; 3 KCl; 1.2 $KH_2PO_4$, 1 $MgSO_4$, 2 $CaCl_2$; 26 $NaHCO_3$; 10 glucose, bubbled with 95% $O_2$–5% $CO_2$ (pH 7.4). The flow rate was kept at 1.5 ml $min^{-1}$ by means of a peristaltic pump (Minipuls 3, Gilson, Villiers, France), and bath temperature was maintained at 30–32°C by an in-line solution heater and temperature controller (TC-344B, Warner Instruments, Hamden, CT, USA).

MVNn were identified with a 40× water immersion objective on an upright microscope equipped with differential interface contrast optics under infrared illumination (BX51WI, Olympus, Tokyo, Japan) and video observation (C3077-71 CCD camera, Hamamatsu Photonics, Japan).

Current- and voltage-clamp recordings were made from neurons in both magnocellular and parvicellular divisions of the MVN (Paxinos & Watson, 1998) with a MultiClamp 700A amplifier (Molecular Devices, Sunnyvale, CA, USA). Only MVNn having interspike membrane potential more negative than −50 mV and spike amplitude higher than 45 mV were used for experiments. Electrodes were made using borosilicate glass micropipettes (Warner Instruments, Hamden, CT, USA) prepared with a P-97 Flaming-Brown micropipette puller (Sutter Instruments, Novato, CA, USA). Pipettes were filled with an internal solution containing (mM): 145 K-gluconate, 2 $MgCl_2$, 0.1 EGTA, 2 $Na_2ATP$ and 10 Hepes (pH 7.2 with KOH; 290 mosmol $l^{-1}$ adjusted with sucrose). The resistance of pipettes filled with this solution was 3–5 MΩ. Access resistance was monitored throughout the entire duration of the recording and was typically <15 MΩ. Data were not corrected for the liquid junction potential (−16 mV).

In a set of experiments aimed at studying the spontaneous firing of MVNn, the perforated-patch configuration was used. For these recordings, gramicidin (Sigma) was added to the pipette solution (the same as in whole-cell recordings) at 10 $\mu$g $ml^{-1}$. Gramicidin was first dissolved in dimethylsulphoxide (DMSO) to a concentration of 10 mg $ml^{-1}$ and it was freshly made every 2 h. Stock solutions were then diluted in the pipette solution just before use. Before backfilling the pipette with the gramicidin-containing solution, the pipette tip was filled with gramicidin-free pipette solution by a brief immersion. Gigaseals were formed with little or no suction to avoid break-in; perforation began within 5–10 min, developing steadily for the following 10–20 min. The progress of perforation was evaluated by monitoring the access resistance, and when it had reached a steady level around 30 MΩ or lower the recording was started. Access resistance was carefully monitored throughout the experiment, and any neurons in which a sudden drop in this parameter occurred were discarded. In these experiments the shape of action potentials was studied by superimposing the traces recorded before and during application of 8-Br-cGMP. The rate of the membrane depolarization in the interspike intervals was defined as the slope of the straight line drawn between the peak of AHP and the threshold for action potential (Wang & Huang, 2006).

In some experiments membrane input resistance was evaluated in current-clamp mode using series of 600 ms-long hyperpolarizing steps (from −40 pA to −10 pA in 10 pA increments). Input resistance was calculated from the peak voltage achieved at each step before and during application of 8-Br-cGMP. The input resistance values were derived from the linear portion of the intensity-to-voltage ($I$–$V$) relationship as the slope of the linear regression fitting line calculated by using the Clampfit program (pClamp9 software, Molecular Devices). Data acquisition and stimulation protocols were performed by Digidata 1200 Series interface and pClamp 9 software. Data were filtered at 1 kHz and digitized at 10 kHz.

**Statistical analysis.** Data are expressed as means ± S.E.M. Statistical significance was assessed with Student's paired $t$ test. For experiments that included fewer than 12 observations, the Wilcoxon signed-rank test (for paired data) and the Mann–Whitney test (for unpaired data) were used. A $P$ value <0.05 was considered significant.

**Solutions.** Drugs were diluted to working concentrations in oxygenated aCSF before use. A three-way stop-cock connected to the perfusion inlet tube was used to deliver test drug solutions into the chamber containing the brain slice. The following drugs were purchased from Sigma: 8-bromoguanosine 3′,5′-cyclic monophosphate sodium salt (8-Br-cGMP); 8-bromoadenosine 3′,5′-cyclic monophosphate sodium salt (8-Br-cAMP); KT5823; 4-aminopyridine (4-AP); *N*-(2-[*p*-bromocinnamylamino]ethyl)-5-isoquinolinesulphonamide (H89); kynurenic acid; picrotoxin; tetraethylammonium chloride (TEA). L-(−)-*cis*-Diltiazem hydrochloride (LCD) was from Affiniti Research Products (Mamhead, UK). Tetrodotoxin (TTX)

and apamin were purchased from Alomone Laboratories. All stock solutions were made up in distilled water except for KT5823, H89 and picrotoxin, which were dissolved in DMSO.

In all experiments $GABA_A$ and ionotropic glutamate receptors were blocked by continuously perfusing the slice with aCSF containing 100 $\mu$M picrotoxin and 2 mM kinurenic acid, respectively.

All recordings, with the exception of those carried out in perforated-patch configuration, were performed using aCSF containing 1.2 $\mu$M TTX to block voltage-dependent $Na^+$ channels, and a cocktail of different $K^+$-channel blockers (20 mM TEA, 0.5 mM 4-AP and 200 nM apamin) to exclude any effects of cyclic nucleotides on these channels potentially affecting the studied responses.

In low-$Ca^+$ and low-$Na^+$ aCSF (choline-aCSF), concentrations of these two ions were lowered to 0.2 mM and 26 mM, respectively, and choline chloride was added as substitute for equimolar NaCl. In experiments using 3 mM $CdCl_2$, both $KH_2PO_4$ and $MgSO_4$ were removed to avoid their precipitation with cadmium.

## Results

### CNG1 and CNG2 channels are expressed in MVNn

In previous studies we demonstrated in the MVN immunoreactivity for CNG channel subunits A1 and A2 (i.e. the functional components of CNG channels of rod- and olfactory-type, respectively), which was mainly associated with cells exhibiting the morphological features of neurons (Podda *et al.* 2005). To better characterize the distribution of these channels in the MVN neurons, we performed double-immunofluorescence labelling with antibodies against the neuronal marker NeuN and either the CNG1 or CNG2 subunit. Both subunits were expressed throughout the MVN with no appreciable differences between the parvi- and magnocellular areas (Fig. 1). The majority of NeuN-labelled cells were also immunoreactive for CNG1 or CNG2 (Fig. 1*A* and *C*). Since immunoreactivity for these subunits (especially CNG2) was also found in some $NeuN^-$ cells, we repeated the double-labelling experiments with the astrocytic marker GFAP. Co-staining for CNG1 and GFAP was never observed, whereas some astrocytes were immunoreactive for CNG2 (Fig. 1*B* and *D*).

### The cyclic nucleotides, cGMP and cAMP, induce protein kinase-independent membrane depolarization in MVNn

The first set of experiments provided clear immunohistochemical evidence of the presence of CNG1 and CNG2 channels in MVNn. Our next step was to determine whether the activation of these channels influences MVNn excitability. CNG1 are activated primarily by direct binding of cGMP, whereas the CNG2 type is equally sensitive to physiological concentrations of cAMP and cGMP (Liman & Buck, 1994; Wei *et al.* 1998; Craven & Zagotta, 2006). Therefore, we performed whole-cell patch-clamp experiments on MVN-containing brainstem slices to characterize the effects on membrane potential of membrane-permeant analogues of cGMP and cAMP (8-Br-cGMP and 8-Br-cAMP).

In current-clamp recordings, hyperpolarizing currents were injected to hold the MVNn membrane potential between $-60$ mV and $-70$ mV (mean $-63.6 \pm 1.3$ mV, $n = 16$), and slices were perfused for 5–7 min with the aCSF containing 1 mM 8-Br-cGMP. Membrane depolarization of $8.9 \pm 0.8$ mV was observed in 13 of the 16 neurons tested (Fig. 2*A* and *B*; $P < 0.001$), with peak effects 5–10 min after drug application. A washout of 15–20 min was usually needed to restore control values, and in some cases the recovery was incomplete. To test the specificity of these responses and their possible dependence on the length of recordings, control experiments were performed in which MVNn membrane potential was recorded for 30–40 min during slice perfusion with aCSF without 8-Br-cGMP. In these experiments ($n = 3$) and in the three cells in which 8-Br-cGMP was ineffective no significant changes in membrane potential were observed.

Bath application of 8-Br-cAMP (1 mM) caused membrane depolarization of $9.2 \pm 1.0$ mV in six out of seven cells tested (Fig. 2*A* and *B*; $P < 0.05$) starting from a control membrane potential of $-60.7 \pm 1.5$ mV. The time course and magnitude of the effects were very similar to those observed with 8-Br-cGMP.

To evaluate the involvement of protein kinase activation in these responses, we repeated the experiments in the presence of selective inhibitors of either protein kinase G, PKG (KT5823, 1 $\mu$M for 30 min) or PKA (H89, 1 $\mu$M for 30 min). As shown in Fig. 2*B*, neither of these drugs prevented the cyclic nucleotide-induced effects on membrane potential ($V_m$). Indeed, 8-Br-cGMP and 8-Br-cAMP induced membrane depolarization of $7.7 \pm 0.6$ mV ($n = 6$) and $9.0 \pm 1.9$ mV ($n = 6$) in the presence of KT5823 and H89, respectively. The effects produced by the cyclic nucleotides on MNVn thus appeared to be a direct action that is not mediated by the activation of protein kinases.

To determine whether cGMP's effects on $V_m$ were due to activation or inhibition of ionic conductances in MVNn, we performed additional current-clamp recordings to assess changes in membrane input resistance associated with membrane depolarization. When the 8-Br-cGMP-induced depolarization had fully developed, hyperpolarizing currents were injected to restore the baseline membrane potential. Starting from this holding current level, the intensity-to-voltage ($I$–$V$) protocols

were applied and input resistance was calculated as described in Methods. Figure 2*C* shows voltage traces and *I–V* plots obtained before and during 8-Br-cGMP exposure in a representative neuron. In this cell, input resistance decreased from 391 MΩ to 306 MΩ after 8-Br-cGMP application. Similar decreases ($19.7 \pm 0.8\%$) were observed in all cells tested (from $354.2 \pm 27.2$ MΩ to $285.0 \pm 22.9$ MΩ, $n = 7$; $P < 0.05$; Fig. 2*D* and *E*). The drop in input resistance documented in these experiments indicates that 8-Br-cGMP-induced depolarization is mediated by ion channel opening.

### Ionic conductances underlying cyclic nucleotide-induced membrane depolarization of MVNn

Voltage-clamp recordings were then made to investigate the nature of the cyclic nucleotide-gated ionic conductance responsible for MVNn depolarization. In MVNn held at −60 mV, exposure to 1 mM 8-Br-cGMP or 1 mM 8-Br-cAMP induced tonic inward currents with mean amplitudes of $-22.2 \pm 3.9$ pA ($n = 16$) and $-21.2 \pm 3.5$ pA ($n = 12$), respectively (Fig. 3*A* and *B*). Current-to-voltage curves based on data collected before

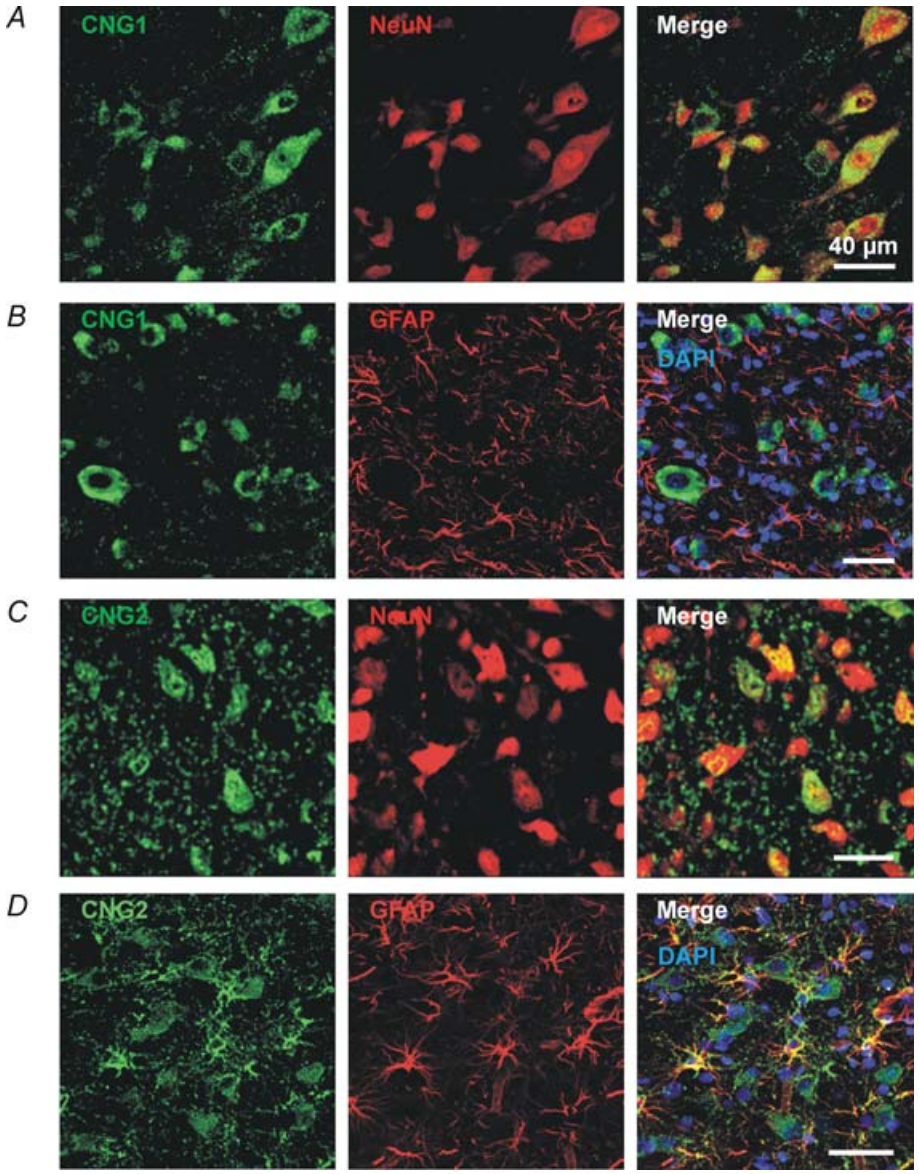


**Figure 1. Expression patterns of CNG1 and CNG2 in coronal sections of MVN**
*A*, CNG1 immunolabelling (green) of MVN neurons identified on the basis of immunoreactivity for NeuN (red). The right panel shows co-localization of the two markers in the majority of the MVNn. *B*, astrocytes ($GFAP^+$ cells, red) do not express CNG1. *C* and *D*, staining for CNG2 (green) is observed in both neurons and astrocytes of the MVN. In the right panels of *B* and *D*, staining of cell nuclei with DAPI (blue) is also shown.

and during the application of 8-Br-cGMP were analysed to determine the reversal potential of these currents. Membrane potential was increased in 10 mV steps to voltages ranging between −80 mV and −30 mV from a holding potential of −60 mV. The net current activated by cGMP was measured by subtracting the current recorded under control conditions from that recorded in the presence of the drug (Fig. 3*C*). The relationship between the voltages and amplitudes of the cGMP-activated currents was apparently monotonic, indicating that the underlying conductance is voltage independent within the range of potentials tested. A linear regression curve was reliably fitted to the data, and the extrapolated reversal potential was found to be 3.0 mV ($n = 5$), a figure that is compatible with the opening of non-selective cation channels such as CNG channels.

To asses the ion selectivity of the channels activated by cGMP, we repeated our experiments with a modified aCSF in which the $Ca^{2+}$ concentration had been decreased to 0.2 mM and the NaCl replaced with equimolar concentrations of choline-Cl (choline-aCSF). These experimental conditions almost completely abolished the cGMP-activated currents ($n = 5$; Fig. 3*C*). In another set of experiments, aCSF was replaced with choline-aCSF after the response to 8-Br-cGMP had fully developed. The result was a marked inhibition of the inward currents (−4.1 ± 1.9 pA *versus* −26.5 ± 5.7 pA in controls; $n = 7$; $P < 0.01$; Fig. 3*D*). The reversal potential, voltage

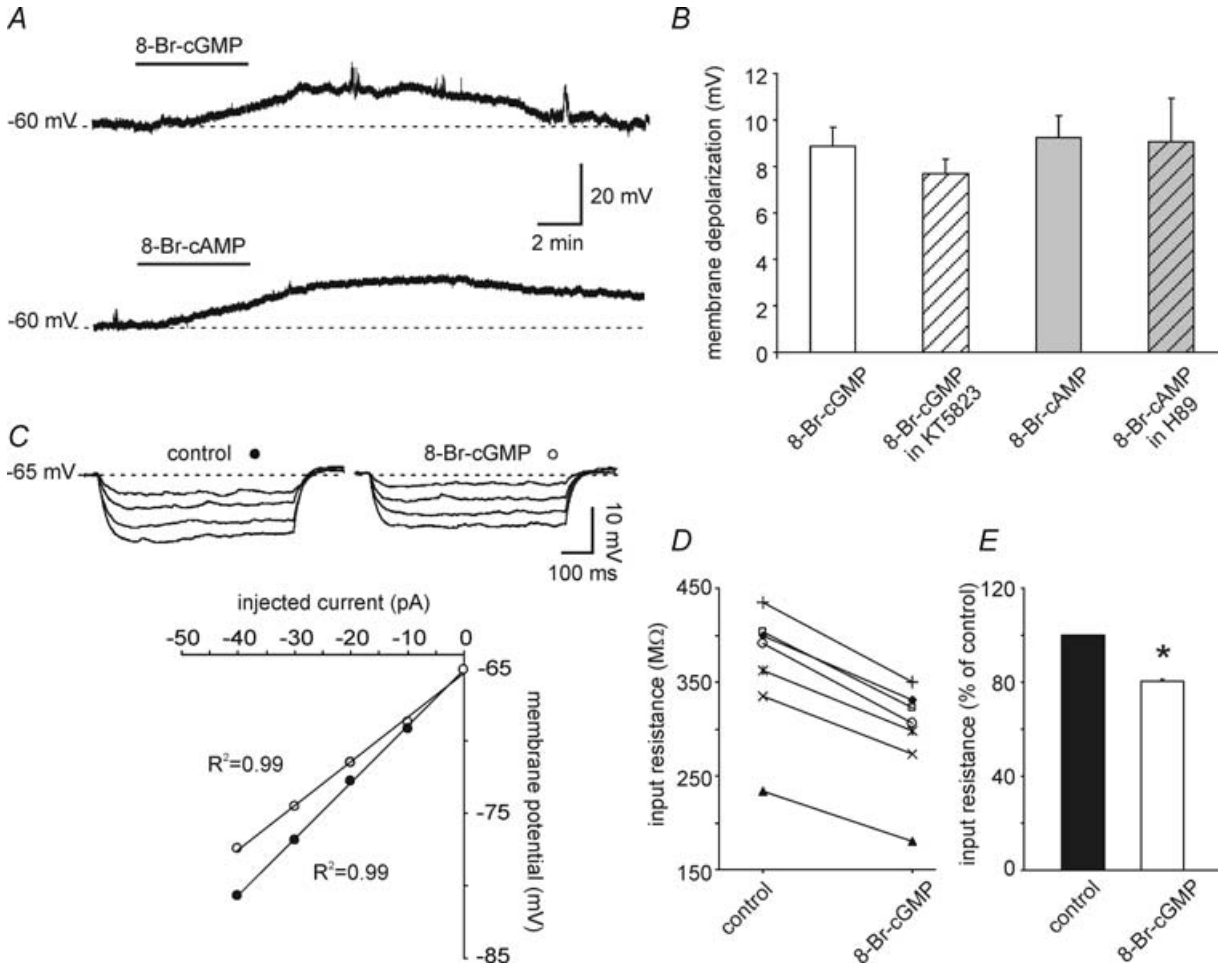


**Figure 2. Effects of cyclic nucleotides on membrane potential of MVNn**
*A*, whole-cell current-clamp recordings showing representative examples of membrane depolarization induced by 1 mM 8-Br-cGMP (top) and 1 mM 8-Br-cAMP (bottom). *B*, mean values of effects induced by 8-Br-cGMP and 8-Br-cAMP alone and in the presence of inhibitors of PKG (KT5823, 1 $\mu$M) and PKA (H89, 1 $\mu$M). *C*, voltage traces (top) and *I–V* curves (bottom) from a representative MVNn subjected to 600 ms hyperpolarizing current steps (from −40 pA to −10 pA in 10 pA increments) in control and during 8-Br-cGMP application. The input resistance of this cell, determined from the slope of linear regression analysis (continuous line), was 391 MΩ in control and 306 MΩ during 8-Br-cGMP application. *D*, plots of input resistance values in all cells tested ($n = 7$) in control conditions and during 8-Br-cGMP application. *E*, input resistance decrease induced by 8-Br-cGMP expressed as percentage of control values. Error bars show S.E.M. values $^*P < 0.05$.

independence, and ion selectivity of the cGMP-gated currents documented in these experiments are fully compatible with the functional properties of CNG channels (Kaupp & Seifert, 2002).

Ion-substitution experiments carried out in current-clamp mode confirmed the effects of decreased extracellular $Na^+$ and $Ca^{2+}$: under the conditions described above, cGMP-induced depolarization was almost completely abolished ($1.6 \pm 0.5$ mV; $n = 5$; $P < 0.001$; Fig. 4*D*).

### Pharmacological characterization of the cyclic nucleotide-induced effects

The effects of cGMP were then tested in the presence of the CNG-channel blocking agents, $Cd^{2+}$ and LCD (Kaupp & Seifert, 2002). Bath application of 3 mM $Cd^{2+}$ abolished the effects of the cyclic nucleotide on the MVNn membrane potential: cGMP-induced changes in $V_m$ had mean amplitudes of $9.5 \pm 1.6$ mV and $-0.5 \pm 0.9$ mV before and after application of $Cd^{2+}$ ($n = 5$; $P < 0.01$; Fig. 4*A* and *B*). Slice perfusion (for 10–15 min) with the more selective CNG channel antagonist, LCD, produced membrane hyperpolarization amounting to $-6.9 \pm 2.5$ mV ($n = 6$; $P < 0.005$). Depolarizing currents were injected to reverse the hyperpolarization and restore $V_m$ values as close as possible to those of controls, and 8-Br-cGMP was then added to the bath. In the presence of LCD, the cyclic nucleotide analogue produced very small membrane depolarizations ($1.4 \pm 0.5$ mV; $n = 6$) that were significantly smaller than those observed in the absence of CNG-channel blockade ($P < 0.001$; Fig. 4*C* and *D*).

Another set of experiments was carried out to determine whether the effects reported above were in any way dependent on the activation of other types of cyclic nucleotide-modulated channels. Cyclic nucleotides are known to enhance the $Na^+/K^+$ current ($I_h$) by modulation of hyperpolarization-activated cyclic nucleotide-modulated (HCN) channels (Robinson & Siegelbaum, 2003). The contribution of $I_h$ to the cGMP-induced membrane depolarization was investigated with the specific HCN-channel blocker, ZD7288 (Gasparini & Di Francesco, 1997). Slice perfusion with 25 $\mu$M ZD7288 for 10–15 min did not significantly affect the membrane potential of MVNn ($V_m = -62.2 \pm 0.8$ mV *versus* $-63.5 \pm 0.4$ mV in

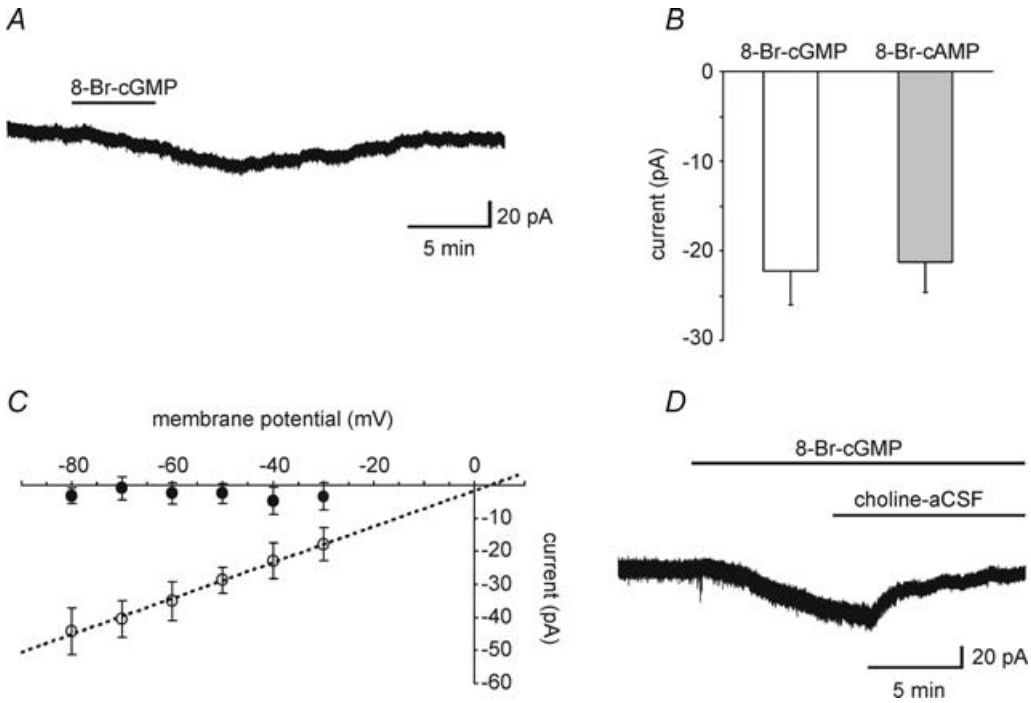


**Figure 3. Cyclic nucleotide-gated currents in MVNn**
*A*, representative inward current elicited by 1 mM 8-Br-cGMP in a MVNn held at −60 mV. *B*, mean amplitude of currents induced by 8-Br-cGMP and 8-Br-cAMP at −60 mV. *C*, *I–V* relationships built plotting data collected from slices perfused with 8-Br-cGMP in aCSF (○) or choline-aCSF (●). Net currents activated by cGMP at the various voltages were obtained by subtracting the currents recorded in control conditions to those recorded in the presence of the 8-Br-cGMP. Voltage steps (from −80 mV to −30 mV in 10 mV increments) were applied from holding potential of −60 mV. Data of cGMP-activated currents recorded in aCSF were fitted by linear regression line ($R^2 = 0.99$, $P < 0.001$). The estimated reversal potential (3.0 mV) was determined by extrapolation. *D*, representative trace showing inhibition of cGMP-activated current following replacement of aCSF with choline-aCSF. Error bars show S.E.M. values

controls; $n = 5$; $P > 0.05$), and it failed to prevent the membrane depolarization induced by the subsequent application of 8-Br-cGMP ($7.1 \pm 0.4$ mV; Fig. 4*D*).

### Effects of CNG channel activation on MVNn spontaneous firing

The data reported thus far strongly suggest that CNG channel activation is responsible for the MVNn responses to cGMP. Our next step therefore was to characterize the potential impact of CNG channel activation on the excitability of spontaneously firing MVNn. In perforated-patch recordings, MVNn exhibited spontaneous overshooting action potentials with mean frequencies of $12.4 \pm 1.0$ Hz ($n = 5$; Fig. 5*A*). Application of 8-Br-cGMP induced membrane depolarization that was associated with significant increases in the MVNn firing rate ($+ 31.7 \pm 4.6\%$; $n = 5$; $P < 0.001$; Fig. 5). To determine whether these increases were caused by $V_m$ modification alone or also by changes in the action potential properties, we compared neuronal discharge measured under control conditions and at the peak of 8-Br-cGMP-induced effects. In the latter case, MVNn firing was also measured during the injection of hyperpolarizing currents, compensating for $V_m$ changes induced by cGMP. Under this condition, the MVNn firing frequency was almost identical to that of controls (Fig. 5*A* and *B*), as were the shape of the action potentials, including AHP, and the slope of the interspike membrane depolarization (Fig. 5*C* and *D*). In contrast, in the absence of hyperpolarizing currents, the slope of the interspike depolarization was significantly increased by 8-Br-cGMP ($0.24 \pm 0.04$ *versus* $0.19 \pm 0.04$ mV ms$^{-1}$ in controls; $n = 5$, $P < 0.005$; Fig. 5*E*). These data indicate that the increased firing rate induced by CNG channel activation is entirely due to membrane depolarization.

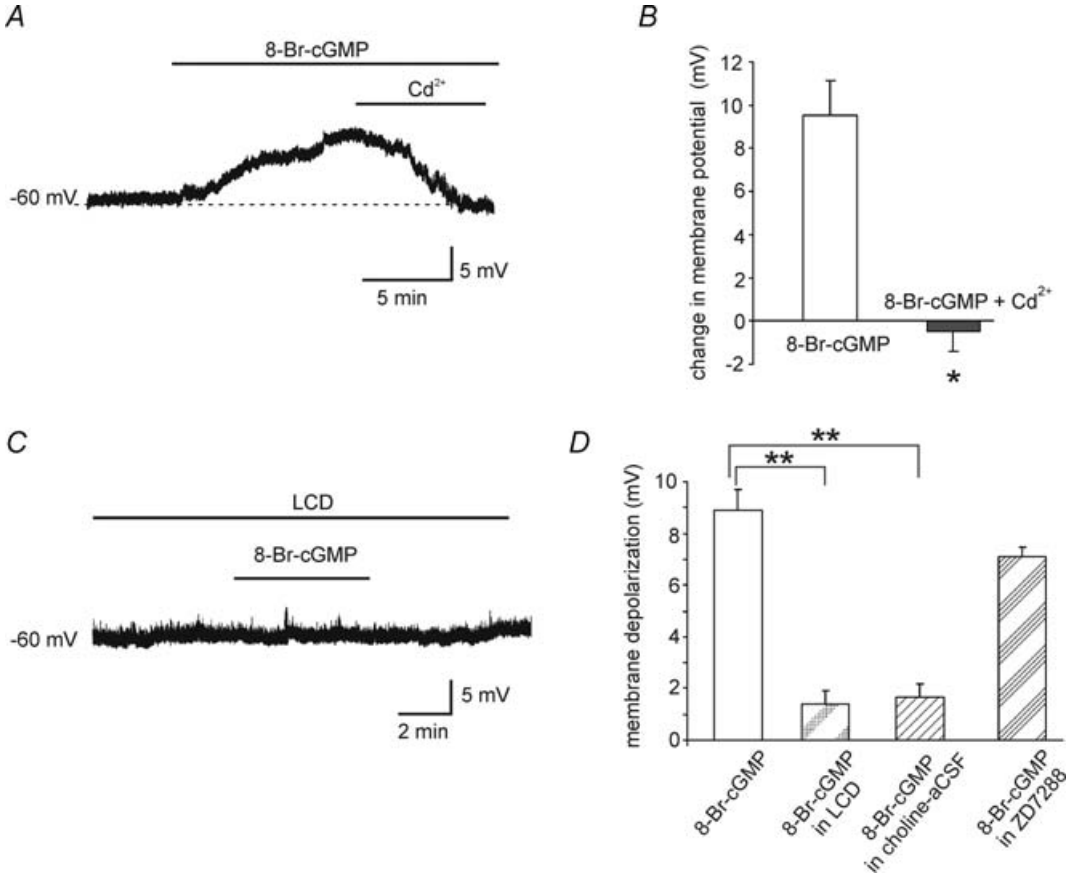


**Figure 4. Effects of CNG and HCN channel blockers on 8-Br-cGMP-induced depolarization**
*A*, application of 3 mM $Cd^{2+}$ reverted the effects of 8-Br-cGMP on $V_m$. *B*, inhibitory effects of $Cd^{2+}$ on 8-Br-cGMP-induced membrane depolarizations in the five studied MVNn. *C*, representative trace showing the lack of 8-Br-cGMP effect in the presence of the CNG channel blocker LCD. *D*, mean values of membrane depolarizations induced by 8-Br-cGMP alone ($n = 13$) and in the presence of: the selective CNG channel blocker LCD (100 $\mu$M; $n = 6$); choline-aCSF ($n = 5$); and the selective HCN channel blocker ZD7288 (25 $\mu$M; $n = 5$). Error bars show S.E.M. values $^*P < 0.05$; $^{**}P < 0.001$.

## Discussion

The present study provides novel evidence that CNG channel activity influences the excitability of MVNn. Cyclic GMP and cAMP induced significant increases in the spontaneous firing rates of these neurons, and this effect was shown to be caused exclusively by membrane depolarization mediated by the activation of voltage-independent, non-inactivating inward currents. The estimated reversal potential of these currents (close to 0 mV) is compatible with non-selective cationic conductance, and both the currents and the membrane depolarization induced by the cyclic nucleotides proved to be dependent on the presence of $Na^+$ and $Ca^{2+}$ in the extracellular medium. The electrophysiological responses we observed in MVNn exposed to cyclic nucleotide analogues are consistent with the functional properties of CNG channels in sensory and CNS neurons (Nawy & Jahr, 1991; Ahmad *et al.* 1994; Leinders-Zufall *et al.* 1995; Bradley *et al.* 1997; for review, see Kaupp & Seifert, 2002). Finally, the effects of cGMP on $V_m$ were almost completely abolished by the CNG-channel blockers, $Cd^{2+}$ and LCD (Haynes, 1992; Charles *et al.* 2001).

Our electrophysiological data are in agreement with the results of our immunohistochemical studies, which demonstrated widespread distribution of both CNG1 and CNG2 subunits throughout the MVN, and their predominant localization in cells expressing the neuronal marker NeuN (Mullen *et al.* 1992). Immunoreactivity for CNG1 and CNG2 subunits was observed in the vast majority of $NeuN^+$ cells, although a few displayed no immunohistochemical evidence of either CNG channel type. This latter finding was consistent with the absence of electrophysiological responses to cyclic nucleotides observed in a few of the MVNn tested. CNG-subunit labelling was also found in a small number of $NeuN^-$ cells. Double-labelling experiments with antibodies against CNG channels and GFAP revealed CNG2, but not CNG1,

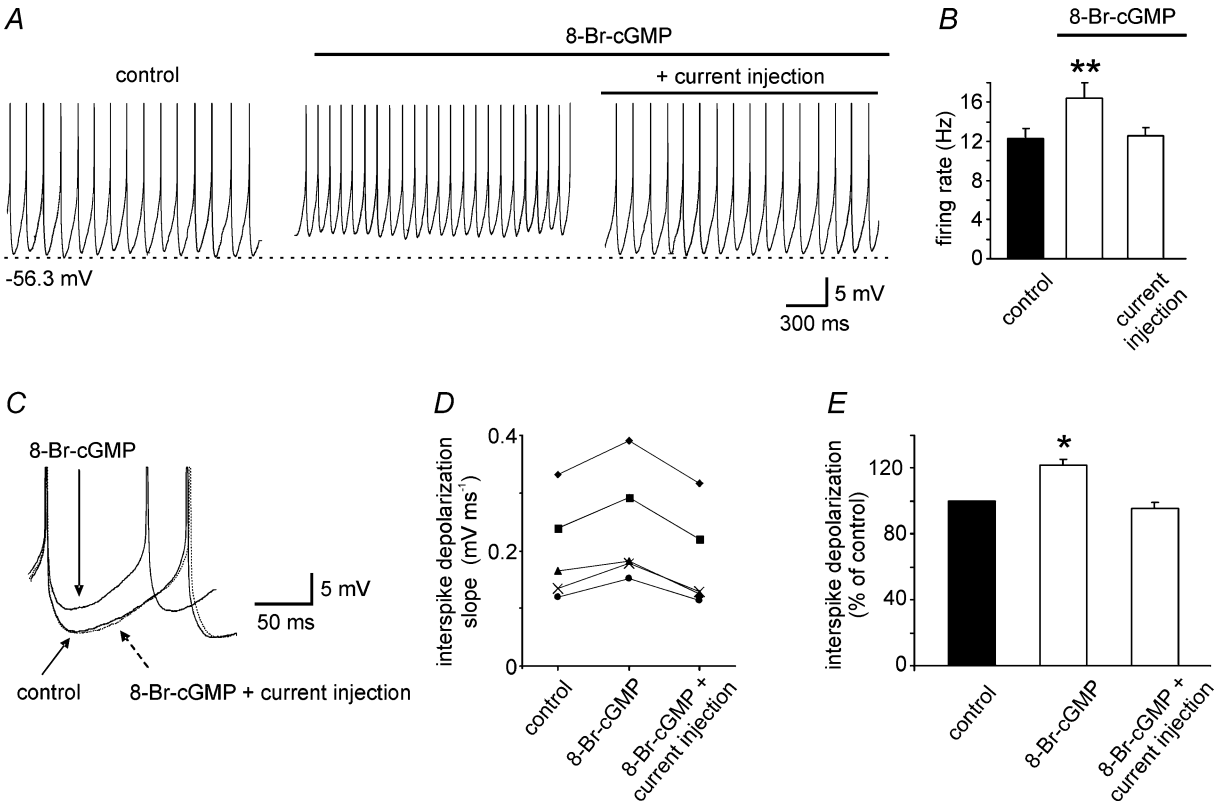


**Figure 5. Effects of 8-Br-cGMP on MVNn firing rate**
*A*, in perforated-patch recordings 1 mM 8-Br-cGMP induced membrane depolarization associated with increase in the discharge frequency (middle trace). The 8-Br-cGMP effects were completely reversed by constant injection of hyperpolarizing currents, returning $V_m$ to the predrug level value (right). Spikes were truncated at −30 mV for clarity. *B*, mean values of the firing rate in control conditions and during 8-Br-cGMP application with and without constant current injection in order to return the membrane potential to control value ($n = 5$). *C*, traces taken from the three conditions shown in *A* are superimposed according to their firing threshold to compare the shape of action potentials. The rate of the membrane depolarization in the interspike intervals was defined as the slope of the straight line drawn between the peak of AHP and the threshold for action potential. Values of interspike depolarization slopes are plotted in *D* and their changes expressed as a percentage of controls in *E*. Error bars show S.E.M. values $^*P < 0.05$.

staining of several astrocytes. With regard to CNG1 labelling of NeuN$^-$ cells, it may be due to the expression of CNG1 by immature neurons or non-astrocytic glial cells (e.g. oligodendrocytes). Identification of the functional role of CNG channels in glial cells was beyond the scope of the present study, but studies are currently underway in our laboratory to address this issue, which is likely to have important physiological implications.

CNG1 and CNG2 expression patterns in MVNn were similar in terms of intensity and distribution, and this finding is supported by our electrophysiological demonstration of the responsiveness of most MVNn to both cGMP and cAMP. The former nucleotide activates all CNG channel subtypes, whereas the CNG2 subunit of the olfactory-type CNG channels is also sensitive to cAMP (Bradley *et al.* 1994; Liman & Buck, 1994; Wei *et al.* 1998; Craven & Zagotta, 2006). Expression of both CNG1 and CNG2 subunits within the MVN was also demonstrated in our previous studies by means of Western blotting and RT-PCR (Podda *et al.* 2004, 2005).

The data discussed above strongly suggest that the inward currents and membrane depolarization induced in MVNn by cyclic nucleotides are mediated by the activation of CNG channels. On the other hand, effects similar to those we documented can admittedly be mediated by other classes of ion channels that are gated or modulated by cyclic nucleotides, either directly or through protein kinase-activated pathways. The latter mechanism was clearly excluded by the results of experiments performed in the presence of selective blockers of PKG and PKA (KT5823 and H89, respectively). These findings are also in line with extracellular MVNn recordings obtained in our previous studies, which show that the firing rate increases induced by activation of the nitric oxide/cGMP pathway or by cAMP are not dependent on protein kinases (Podda *et al.* 2004, 2005). The possible contribution of voltage-gated $Na^+$ and $K^+$ currents to the studied responses should be also considered. Their modulation by cyclic nucleotides has been described in invertebrate neurons (Connor & Hockberger, 1984; Sawada *et al.* 1995), and more recently, it has been suggested that cGMP-mediated inhibition of $Ca^{2+}$-dependent $K^+$-conductances might be responsible for the excitatory effects of nitric oxide in freshly isolated MVNn (Kim *et al.* 2004). It is unlikely, however, that this mechanism played any role in the effects we observed since, with the exception of data related to spontaneous MVNn firing, all of our findings are based on experiments performed in the presence of $Na^+$ and $K^+$ channel blockers, including TTX, TEA, 4-AP and apamin. In addition, the cGMP-induced depolarization was associated with a significant decrease in membrane input resistance that excludes the contribution of $K^+$ current inhibition to the effects we observed. The possible involvement of cyclic nucleotide-induced modulation of other inward cationic currents can also be ruled out since our experimental protocol included the blockade of voltage-gated $Na^+$ channels and glutamate ionotropic receptors. These experimental conditions, together with $GABA_A$ receptor blockade, also isolated the MVNn from synaptic inputs, whose involvement in the observed effects can thus be excluded (Murphy & Isaacson, 2003; Barnstable *et al.* 2004).

The HCN channels might also be responsible for the effects we observed. Their hyperpolarization-dependent activation is markedly increased by cAMP and, to a much lesser extent, by cGMP, and these modulatory effects contribute to the regulation of excitability of several types of neurons (Robinson & Siegelbaum, 2003; Baruscotti & Di Francesco, 2004). These non-selective cationic channels, activated at $V_m$ values more negative than the resting membrane potential, produce slow membrane depolarization and rescue $V_m$ from conditions of hyperpolarization, which preclude the activation of voltage-dependent cationic inward currents responsible for triggering action potential. Their function is therefore crucial for pacemaking mechanisms underlying the spontaneous firing of different excitable cells. Although HCN channels are expressed in MVNn (Notomi & Shigemoto, 2004), they do not appear to contribute to the generation or the regulation of the spontaneous activity of these neurons (Sekirnjak & du Lac, 2002; Straka *et al.* 2005). This conclusion is in line with our demonstration that the selective HCN blocker ZD7288 (Gasparini & Di Francesco, 1997) did not significantly affect MVNn $V_m$. The persistence of cGMP effects in the presence of HCN channel blockade excludes the involvement of these channels in the MVNn responses to cyclic nucleotides reported here. Previous reports have already highlighted the widespread expression of CNG channels within the CNS. PCR and *in situ* hybridization studies have demonstrated their presence in the hippocampus, cerebellum, cerebral cortex, and brainstem of rats (el-Husseini *et al.* 1995; Kingston *et al.* 1996, 1999; Bradley *et al.* 1997; Samanta Roy & Barnstable, 1999; Strijbos *et al.* 1999). Their broad distribution within the brain strongly suggests that CNG channels' functional roles are not confined to sensory signal transduction like that occurring in photoreceptors and olfactory receptors, where these channels were first identified (Fesenko *et al.* 1985; Dhallan *et al.* 1990; Kaupp & Seifert, 2002; Ko *et al.* 2004). As mentioned above, most of the studies on CNG channels in the CNS have been based on molecular techniques, and very few electrophysiological investigations have examined the effects of their activation in CNS neurons. These studies were carried out in rat hippocampal neurons and pituitary neuroendocrine cells. Voltage-independent cationic currents activated by cyclic GMP, and to a lesser extent by cAMP, were recorded in isolated hippocampal neurons in culture (Leinders-Zufall *et al.* 1995; Bradley *et al.* 1997). These currents were blocked by application

of the divalent cations $Mg^{2+}$ and $Cd^{2+}$, and inhibited by high extracellular $Ca^{2+}$ concentrations. In hippocampal slices, CNG channels have been proposed to contribute to the plateau potentials induced by muscarinic receptor activation in CA1 pyramidal neurons (Kuzmiski & MacVicar, 2001). Finally, activation of CNG channels by either cAMP or different neurotransmitters stimulating the cAMP production has been reported to increase the frequency of $Ca^{2+}$ oscillations in immortalized hypothalamic neurons, thus contributing to regulation of the spontaneous release of gonadotropin-releasing hormone (Charles *et al.* 2001).

Our demonstration that CNG channels influence MVNn excitability takes us one step closer towards a functional characterization of these channels within the CNS. One of the goals of cellular neurophysiology is a better understanding of the mechanisms that regulate neuronal excitability and the multiple ionic conductances that determine the resting membrane potential (RMP). Various voltage-dependent and voltage-independent conductances have been proposed as possible RMP determinants (Crill, 1996; Goldstein *et al.* 2001; Robinson & Siegelbaum, 2003; Lu *et al.* 2007), but the issue is far from being resolved. Identification of the ionic conductances that influence the RMP is particularly important for spontaneously active neurons like those of the MVN (Straka *et al.* 2005; Gittis & du Lac, 2007). The RMP is the foundation upon which voltage-dependent subthreshold and suprathreshold currents exert their effects. Neuronal pacemaking activity requires ion channel opening at subthreshold voltages, i.e. at membrane potentials lower than those that trigger firing action potentials (Robinson & Siegelbaum, 2003; Baruscotti & Di Francesco, 2004; Jackson *et al.* 2004). The currents entering the cell through these channels depolarize the membrane, bringing it closer to the threshold for action potential firing. We propose that CNG channels play a significant role in determining and/or regulating the membrane potential of MVNn, which obviously has a profound impact on their spontaneous, subthreshold depolarizations. In this manner, CNG channels can contribute to the modulation of MVNn action potential firing. This action of CNG channels, which is probably not confined to MVNn, could represent a broad mechanism for modulating the RMP and, consequently, the excitability of neurons in different brain areas.

CNG channels are directly activated by cyclic nucleotides, which can be tonically produced in some neurons (Kretschmannova *et al.* 2006; Ding *et al.* 2007; Tanaka *et al.* 2007). Therefore, it seems reasonable to assume that these channels will be tonically activated in MVNn, a hypothesis that is also consistent with the membrane hyperpolarization we observed following CNG channel blockade. Moreover, the level of CNG channel activity can change in response to the activation of neurotransmitter receptors linked to cyclic nucleotide production or the modulation of enzymes responsible for their degradation. A pathway for cGMP production involving activation of soluble guanylyl cyclase by nitric oxide has been clearly demonstrated in the MVN (Podda *et al.* 2004), and various groups have shown that MVNn firing rates can be modulated by neurotransmitters that modify intracellular levels of cyclic nucleotides (Lin & Carpenter, 1993; Johnston *et al.* 1994; de Waele *et al.* 1995; Podda *et al.* 2001).

In summary, we have demonstrated that CNG channels are the target of cyclic nucleotides in MVNn and that their activation significantly contributes to regulation of the spontaneous firing of these neurons. This effect is not associated with changes in the ionic conductances responsible for MVNn pacemaking activity or in action potential shape: it is caused exclusively by CNG channel-mediated membrane depolarization.

The functional implications of this regulatory mechanism are potentially far-reaching. The firing behaviour of MVNn has a major impact on their ability to integrate the sensory inputs converging onto them and to elaborate output signals to their targets. Moreover, it would be interesting to determine the contribution of CNG channels to the maturation of MVNn membrane properties occurring during the postnatal period, and particularly that associated with the time of the first eye opening (around postnatal day P13). The major changes in the biophysical properties of mouse MVNn occur between P10 and P15, and these neurons reach their electrophysiological maturity between P15 and P30 (Johnston & Dutia, 1996; Dutia & Johnston, 1998). Although our patch-clamp recordings were performed from neurons of P14–P17 rats showing membrane potential values and firing discharges at rest comparable with those of young adult animals, we cannot exclude that some neurons included in our study were not fully mature. It is tempting to speculate that the absence of electrophysiological responses to cyclic nucleotides we observed in few MVNn, as well as the lack of immunoreactivity for CNG in some $NeuN^{+}$ cells, could reflect differences in the expression of CNG channels between mature and immature MVNn. Finally, modulation of CNG channel activity could play a role in the pathophysiological modifications of MVNn membrane properties that have been associated with the behavioural plasticity of gaze and posture control (Murphy & du Lac, 2001; Straka *et al.* 2005). In particular, the process of vestibular compensation, i.e. the behavioural recovery occurring after unilateral vestibular de-afferentation is associated with plastic changes of the intrinsic active and passive membrane properties of MVNn as well as with changes in their discharge behaviour and sensitivity to neurotransmitters. Changes in the expression of CNG channels or in the intracellular levels of cyclic nucleotides might

play significant roles in the induction and/or progression of the processes underlying vestibular system plasticity. A modulatory action exerted by the histaminergic system on neurotransmission in the MVN, and its changes during vestibular compensation, have been recently reported (Bergquist *et al.* 2006; Tighilet *et al.* 2006). Activation of histamine $H_2$ and $H_3$ receptors mediating these effects modifies the intracellular levels of cAMP via G-protein-dependent modulation of adenylyl cyclase activity and, consequently, it has potential influence on CNG channel function.

In conclusion, our findings reveal an important and novel mechanism for regulating MVNn excitability, which is mediated by voltage-independent cationic channels and is potentially operative in various CNS structures.

## References


Ahmad I, Leinders-Zufall T, Kocsis JD, Shepherd GM, Zufall F & Barnstable CJ (1994). Retinal ganglion cells express a cGMP-gated cation conductance activatable by nitric oxide donors. *Neuron* **12**, 155–165.

Barnstable CJ, Wei JY & Wei MH (2004). Modulation of synaptic function by cGMP and cGMP-gated cation channels. *Neurochem Int* **45**, 875–884.

Baruscotti M & Di Francesco D (2004). Pacemaker channels. *Ann N Y Acad Sci* **1015**, 111–121.

Bergquist F, Ruthven A, Ludwig M & Dutia MB (2006). Histaminergic and glycinergic modulation of GABA release in the vestibular nuclei of normal and labyrinthectomised rats. *J Physiol* **577**, 857–868.

Bradley J, Li J, Davidson N, Lester HA & Zinn K (1994). Heteromeric olfactory cyclic nucleotide-gated channels: a subunit that confers increased sensitivity to cAMP. *Proc Natl Acad Sci U S A* **91**, 8890–8894.

Bradley J, Zhang Y, Bakin R, Lester HA, Ronnett GV & Zinn K (1997). Functional expression of the heteromeric 'olfactory' cyclic nucleotide-gated channel in the hippocampus: a potential effector of synaptic plasticity in brain neurons. *J Neurosci* **17**, 1993–2005.

Charles A, Weiner R & Costantin J (2001). cAMP modulates the excitability of immortalized hypothalamic (GT1) neurons via a cyclic nucleotide gated channel. *Mol Endocrinol* **15**, 997–1009.

Chun SW, Choi JH, Kim MS & Park BR (2003). Characterization of spontaneous synaptic transmission in rat medial vestibular nucleus. *Neuroreport* **14**, 1485–1488.

Connor JA & Hockberger P (1984). A novel membrane sodium current induced by injection of cyclic nucleotides into gastropod neurones. *J Physiol* **354**, 139–162.

Craven KB & Zagotta WN (2006). CNG and HCN channels: two peas, one pod. *Annu Rev Physiol* **68**, 375–401.

Crill WE (1996). Persistent sodium current in mammalian central neurons. *Annu Rev Physiol* **58**, 349–362.

D'Ascenzo M, Fellin T, Terunuma M, Revilla-Sanchez R, Meaney DF, Auberson YP, Moss SJ & Haydon PG (2007). mGluR5 stimulates gliotransmission in the nucleus accumbens. *Proc Natl Acad Sci U S A* **104**, 1995–2000.

Dhallan RS, Yau KW, Schrader KA & Reed RR (1990). Primary structure and functional expression of a cyclic nucleotide-activated channel from olfactory neurons. *Nature* **347**, 184–187.

Ding S, Luo JH & Yuan XB (2007). Semaphorin-3F attracts the growth cone of cerebellar granule cells through cGMP signaling pathway. *Biochem Biophys Res Commun* **356**, 857–863.

Dutia MB & Johnston AR (1998). Development of action potentials and apamin-sensitive after-potentials in mouse vestibular nucleus neurones. *Exp Brain Res* **118**, 148–154.

Dutia MB, Johnston AR & McQueen DS (1992). Tonic activity of rat medial vestibular nucleus neurones in vitro and its inhibition by GABA. *Exp Brain Res* **88**, 466–472.

el-Husseini AE, Bladen C & Vincent SR (1995). Expression of the olfactory cyclic nucleotide gated channel (CNG1) in the rat brain. *Neuroreport* **6**, 1459–1463.

Eugène D, Deforges S, Guimont F, Idoux E, Vidal PP, Moore LE & Vibert N (2007). Developmental regulation of the membrane properties of central vestibular neurons by sensory vestibular information in the mouse. *J Physiol* **583**, 923–943.

Fesenko EE, Kolesnikov SS & Lyubarsky AL (1985). Induction by cyclic GMP of cationic conductance in plasma membrane of retinal rod outer segment. *Nature* **313**, 310–313.

Gasparini S & Di Francesco D (1997). Action of the hyperpolarization-activated current ($I_h$) blocker ZD 7288 in hippocampal CA1 neurons. *Pflugers Arch* **435**, 99–106.

Gittis AH & du Lac S (2007). Firing properties of GABAergic versus non-GABAergic vestibular nucleus neurons conferred by a differential balance of potassium currents. *J Neurophysiol* **97**, 3986–3996.

Goldstein SA, Bockenhauer D, O'Kelly I & Zilberberg N (2001). Potassium leak channels and the KCNK family of two-P-domain subunits. *Nature Rev Neurosci* **2**, 175–184.

Haynes LW (1992). Block of the cyclic GMP-gated channel of vertebrate rod and cone photoreceptors by 1-cis-diltiazem. *J Gen Physiol* **100**, 783–801.

Jackson AC, Yao GL & Bean BP (2004). Mechanism of spontaneous firing in dorsomedial suprachiasmatic nucleus neurons. *J Neurosci* **24**, 7985–7998.

Johnston AR & Dutia MB (1996). Postnatal development of spontaneous tonic activity in mouse medial vestibular nucleus neurones. *Neurosci Lett* **219**, 17–20.

Johnston AR, MacLeod NK & Dutia MB (1994). Ionic conductances contributing to spike repolarization and after-potentials in rat medial vestibular nucleus neurones. *J Physiol* **481**, 61–77.

Kaupp UB & Seifert R (2002). Cyclic nucleotide-gated ion channels. *Physiol Rev* **82**, 769–824.

Kim HW, Park JS, Jeong HS, Jang MJ, Kim BC, Kim MK, Cho KH, Kim TS & Park SW (2004). Nitric oxide modulation of the spontaneous firing of rat medial vestibular nuclear neurons. *Pharmacol Sci* **96**, 224–228.

Kingston PA, Zufall F & Barnstable CJ (1996). Rat hippocampal neurons express genes for both rod retinal and olfactory cyclic nucleotide-gated channels: novel targets for cAMP/cGMP function. *Proc Natl Acad Sci U S A* **93**, 10440–10445.

Kingston PA, Zufall F & Barnstable CJ (1999). Widespread expression of olfactory cyclic nucleotide-gated channel genes in rat brain: implications for neuronal signalling. *Synapse* **32**, 1–12.

Ko GY, Ko ML & Dryer SE (2004). Circadian regulation of cGMP-gated channels of vertebrate cone photoreceptors: role of cAMP and Ras. *J Neurosci* **24**, 1296–1304.

Kretschmannova K, Gonzalez-Iglesias AE, Tomic M & Stojilkovic SS (2006). Dependence of hyperpolarisation-activated cyclic nucleotide-gated channel activity on basal cyclic adenosine monophosphate production in spontaneously firing GH3 cells. *J Neuroendocrinol* **18**, 484–493.

Kuzmiski JB & MacVicar BA (2001). Cyclic nucleotide-gated channels contribute to the cholinergic plateau potential in hippocampal CA1 pyramidal neurons. *J Neurosci* **21**, 8707–8714.

Leinders-Zufall T, Rosenboom H, Barnstable CJ, Shepherd GM & Zufall F (1995). A calcium-permeable cGMP-activated cation conductance in hippocampal neurons. *Neuroreport* **6**, 1761–1765.

Liman ER & Buck LB (1994). A second subunit of the olfactory cyclic nucleotide-gated channel confers high sensitivity to cAMP. *Neuron* **13**, 511–621.

Lin Y & Carpenter DO (1993). Medial vestibular neurons are endogenous pacemakers whose discharge is modulated by neurotransmitters. *Cell Mol Neurobiol* **13**, 601–613.

Lu B, Su Y, Das S, Liu J, Xia J & Ren D (2007). The neuronal channel NALCN contributes resting sodium permeability and is required for normal respiratory rhythm. *Cell* **129**, 371–383.

Mullen RJ, Buck CR & Smith AM (1992). NeuN, a neuronal specific nuclear protein in vertebrates. *Development* **116**, 201–211.

Murphy GJ & du Lac S (2001). Postnatal development of spike generation in rat medial vestibular nucleus neurons. *J Neurophysiol* **85**, 1899–1906.

Murphy GJ & Isaacson JS (2003). Presynaptic Cyclic nucleotide-gated ion channels modulate neurotransmission in the mammalian olfactory bulb. *Neuron* **37**, 639–647.

Nawy S & Jahr CE (1991). cCMP-gated conductance in retinal bipolar cells is suppressed by the photoreceptor transmitter. *Neuron* **7**, 677–683.

Notomi T & Shigemoto R (2004). Immunohistochemical localization of $I_h$ channel subunits HCN1–4, in the rat brain. *J Comp Neurol* **471**, 241–276.

Paxinos G & Watson C (1998). *The Rat Brain in Stereotaxic Coordinates*. Academic Press, San Diego.

Podda MV, Johnston AR, Tolu E & Dutia MB (2001). Modulation of rat medial vestibular nucleus neurone activity by vasopressin and noradrenaline in vitro. *Neurosci Lett* **298**, 91–94.

Podda MV, Marcocci ME, Del Carlo B, Palamara AT, Azzena GB & Grassi C (2005). Expression of cyclic nucleotide-gated channels in the rat medial vestibular nucleus. *Neuroreport* **16**, 1939–1943.

Podda MV, Marcocci ME, Oggiano L, D'Ascenzo M, Tolu E, Palamara AT, Azzena GB & Grassi C (2004). Nitric oxide increases the spontaneous firing rate of rat medial vestibular nucleus neurons in vitro via a cyclic GMP-mediated PKG-independent mechanism. *Eur J Neurosci* **20**, 2124–2132.

Robinson RB & Siegelbaum SA (2003). Hyperpolarization-activated cation currents: from molecules to physiological function. *Annu Rev Physiol* **65**, 453–480.

Samanta Roy DR & Barnstable CJ (1999). Temporal and spatial pattern of expression of cyclic nucleotide-gated channels in developing rat visual cortex. *Cereb Cortex* **9**, 340–347.

Sawada M, Ichinose M & Hara N (1995). Nitric oxide induces an increased $Na^+$ conductance in identified neurons of Aplysia. *Brain Res* **670**, 248–256.

Sekirnjak C & du Lac S (2002). Intrinsic firing dynamics of vestibular nucleus neurons. *J Neurosci* **22**, 2083–2095.

Straka H, Vibert N, Vidal PP, Moore LE & Dutia MB (2005). Intrinsic membrane properties of vertebrate vestibular neurons: function, development and plasticity. *Prog Neurobiol* **76**, 349–392.

Strijbos PJ, Pratt GD, Khan S, Charles IG & Garthwaite J (1999). Molecular characterization and in situ localization of a full-length cyclic nucleotide-gated channel in rat brain. *Eur J Neurosci* **11**, 4463–4467.

Tanaka S, Ishii K, Kasai K, Yoon SO & Saeki Y (2007). Neural expression of G protein-coupled receptors GPR3, GPR6, and GPR12 up-regulates cyclic AMP levels and promotes neurite outgrowth. *J Biol Chem* **282**, 10506–10515.

Tighilet B, Trottier S, Mourre C & Lacour M (2006). Changes in the histaminergic system during vestibular compensation in the cat. *J Physiol* **573**, 723–739.

de Waele C, Muhlethaler M & Vidal PP (1995). Neurochemistry of the central vestibular pathways. *Brain Res Brain Res Rev* **20**, 24–46.

Wang YC & Huang RC (2006). Effects of sodium pump activity on spontaneous firing in neurons of the rat suprachiasmatic nucleus. *J Neurophysiol* **96**, 109–118.

Wei JY, Roy DS, Leconte L & Barnstable CJ (1998). Molecular and pharmacological analysis of cyclic nucleotide-gated channel function in the central nervous system. *Prog Neurobiol* **56**, 37–64.

Wilson VJ, Yamagata Y, Yates BJ, Schor RH & Nonaka S (1990). Response of vestibular neurons to head rotations in vertical planes. III. Response of vestibulocollic neurons to vestibular and neck stimulation. *J Neurophysiol* **64**, 1695–1703.

Zufall F, Shepherd GM & Barnstable CJ (1997). Cyclic nucleotide gated channels as regulators of CNS development and plasticity. *Curr Opin Neurobiol* **7**, 404–412.

## Acknowledgements

This work was supported by the Italian Ministry of University and Research and by local funds of the Catholic University.